

Soft Expectation and Deep Maximization for Image Feature Detection

Alexander Mai
University of California, San Diego
9500 Gilman Dr, La Jolla, CA 92093
amai@ucsd.edu

Allen Yang
University of California, Berkeley
Berkeley, CA
yang@eecs.berkeley.edu

Dominique E. Meyer
University of California, San Diego
9500 Gilman Dr, La Jolla, CA 92093
dom@ucsd.edu

Abstract

Central to the application of many multi-view geometry algorithms is the extraction of matching points between multiple viewpoints, enabling classical tasks such as camera pose estimation and 3D reconstruction. Over the decades, many approaches that characterize these points have been proposed based on hand-tuned appearance models and more recently data-driven learning methods. We propose SEDM, an iterative semi-supervised learning process that flips the question and first looks for repeatable 3D points, then trains a detector to localize them in image space. Our technique poses the problem as one of expectation maximization (EM), where the likelihood of the detector locating the 3D points is the objective function to be maximized. We utilize the geometry of the scene to refine the estimates of the location of these 3D points and produce a new pseudo ground truth during the expectation step, then train a detector to predict this pseudo ground truth in the maximization step. We apply our detector to standard benchmarks in visual localization, sparse 3D reconstruction, and mean matching accuracy. Our results show that this new model trained using SEDM is able to better localize the underlying 3D points in a scene, improving mean SfM quality by -0.15 ± 0.11 mean reprojection error when compared to SuperPoint or -0.38 ± 0.23 when compared to R2D2.

1. Introduction

A sparse image feature is a region in image space that corresponds to an object location in world space that can be reliably found and matched across multiple viewpoints. Specifically, our paper looks at keypoints, also known as corner or point features, which are elements $p \in \mathbb{R}^2$ in im-

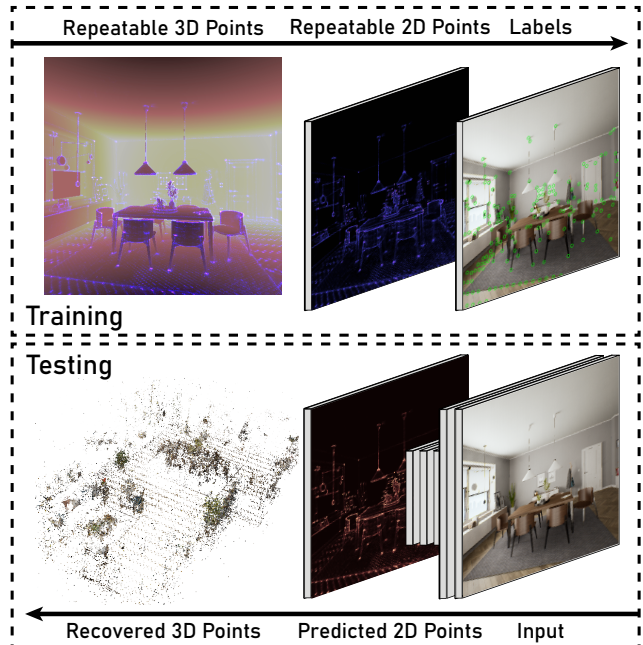


Figure 1. During the training, repeatable points are found and projected into 2D space to create pseudo labels for our detector. Then, during testing, the detector tries to predict the location of these 3D points in 2D space so that these 3D points can be recovered using multi-view geometry.

age space, with the goal of forming point correspondence between multiple images for use in various problems such as finding the relative pose between two perspective images, Structure-from-Motion (SfM), Simultaneous Localization and Mapping (SLAM), and many more [1].

One of the most important aspects of a feature detector is the repeatability of its keypoints, which is essentially a form of self-consistency. Let $I^{(i)} \in \mathbb{R}^{m \times n}$, $i \in 1 \dots N$ be a

sample of images over which we estimate the repeatability of our detector. Let our detector be $f(I^{(i)}) = \{x_j^{(i)}\}_{j=1}^{L_i}$, where $x_j^{(i)} \in \mathbb{R}^2$ is the j th point feature detected. One common way to create a detector is to output a heatmap across the image and select peaks to be the features. Now imagine a simple scenario where all of the images are of the corner of the same box, for which the detector predicts one point, $x_1^{(i)}$, at the corner of the box. The 3D location of this corner would project into each of the images $I^{(i)}$ to get some ground truth location $y^{(i)} \in \mathbb{R}^2$. The error between the predicted and ground truth location, called reprojection error, would be $\|x_1^{(i)} - y^{(i)}\|_2$. The repeatability is the probability that we would detect this same corner within some reprojection error threshold t for any view. In a more general scenario where location of the 3D point underlying the feature is not known, the ground truth location is often estimated by minimizing the sum of the reprojection error across the images in which the feature is detected. A good detector therefore self consistent across a wide array of different scenes from different viewpoints, enabling accurate 3D reconstruction and pose estimation.

1.1. Contributions

In this paper, we propose *Soft Expectation, Deep Maximization* (SEDM), a novel algorithm for optimizing feature repeatability. Given some scene, SEDM searches for a set of repeatable points, which the detector is then trained to predict, as depicted in Figure 1. At test time, the detector would then find features corresponding to some underlying set of 3D points in the scene that could be recovered using SfM. We call this a flipped optimization because it reverses the traditional approach, which was to design a detector that assigns self-consistent scores to the same points in 3D space, resulting in a set of 3D points that will be detected repeatably.

Since the repeatability of a set of points is, by nature, dependent on whether the detector can be trained to predict them, we develop an iterative process that starts with a randomly initialized network and gradually improves the repeatability of the set of points. At each step, SEDM first estimates a soft expected value for the repeatability of points in 3D space, then trains a deep learning detector to predict points that would maximize this repeatability.

Our main contributions are summarized as follows:

- We flip the paradigm of training a feature detector to assign consistent scores to points in 3D space so a set of repeatable set of 3D points can be found and start by finding the repeatable set of 3D points.
- We introduce SEDM, a model agnostic expectation maximization style method that uses this flipped paradigm to train a deep learning feature detector.

- Our benchmarks provide evidence that SEDM is able to improve feature detection when compared to previous state of the art deep learning methods, even when trained on solely synthetic data.

2. Related Work

Methods for detecting image features are typically split into two categories: traditional and deep learning. This split aligns with the difference in the number of parameters to tune, ranging from traditional model-based methods having a few dozen to deep learning methods with millions. FAST [34], which used machine learning to build a decision tree to classify whether a point was a corner (using a manually labeled dataset), is still considered a traditional method by this definition. Of the traditional methods, SIFT [25] remains a gold standard in SfM reconstruction accuracy [42]. When combined with an improved descriptor like HardNet [28] and a guided matcher, SIFT still beats other state-of-the-art methods on leaderboards like the Image Matching Challenge 2020 for 8k features [18].

Deep Learning in Feature Detection. One of the most successful methods, Superpoint [10], has proven very capable when combined with SuperGlue matcher [36]. This combination has won several benchmarks, including the Image Matching Challenge for 2048 features [18] and the Visual Localization Benchmark on several dataset [37]. SuperPoint differs from most other approaches in that it starts with ground-truth 3D geometry with known features. To train MagicPoint, the supervisor of SuperPoint, the method generated a synthetic dataset of simple lines and geometric shapes and labeled the corners as features. MagicPoint is used to supervise SuperPoint so it can learn to predict these same corners under image warping.

Using image warping to approximate viewpoint change is a common method for optimizing towards repeatability between two or more heatmaps, such as in KeyNet [5], Unsuperpoint [8], DetNet [23]. This method can be extended to model nonplanar change of perspective by extracting image patches around keypoints and warping the individual patches, such as in QuadNet [40] and R2D2 [32]. SIPs [9] utilizes point tracking and a sparse loss to perform what could be thought of as a sparse warp. These methods utilize some kind of approximation of projection and reprojection, which likely hinders the accuracy of the detector. LF-Net[29] utilizes the depth to directly back project one heatmap into the space of another, but limit the viewpoint change by only selecting pairs that are temporally adjacent. TILDE [45] optimizes towards repeatability without warping heatmaps by learning on stationary webcams. LIFT [49] filters keypoints output by SIFT using SfM and treats those as ground truth. D2Net [11], ASLFeat [26], and

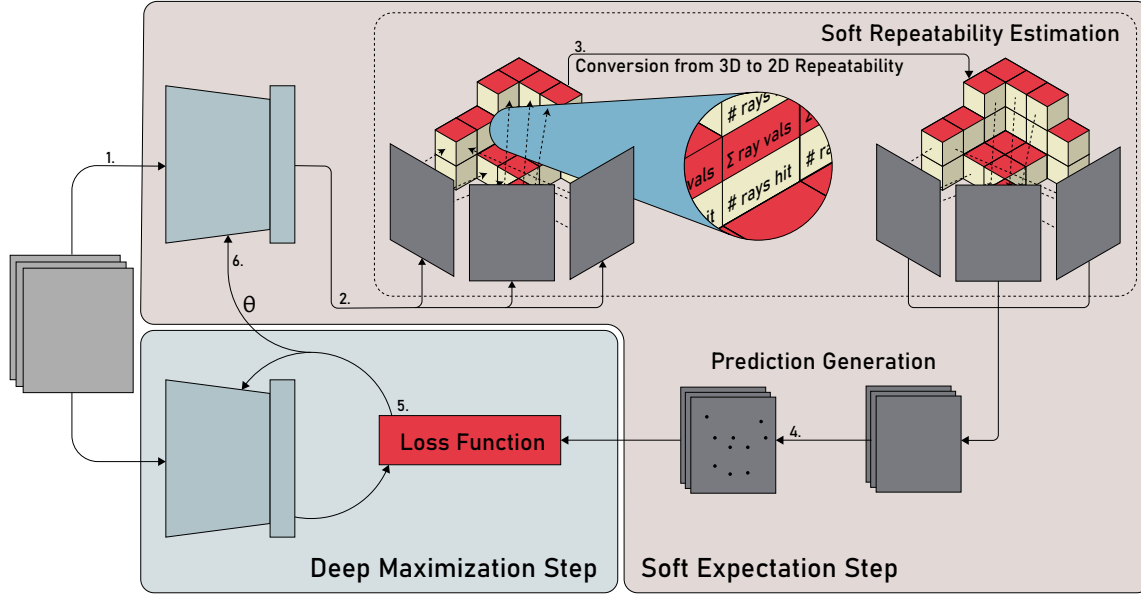


Figure 2. Diagram explaining training process. We start by initializing the network (depicted twice) with random weights. 1. Perform inference on images to generate heatmaps for the location of features in image space. 2. Project heatmap values onto the known voxel map of scene and accumulate the average heatmap value across all viewpoints within all voxels, as seen in the zoom in. 3. Project these soft 3D repeatability values back into image space. 4. Use these soft 2D repeatability values to estimate the optimal features to detect for each image. 5. Minimize the loss function for the model using these estimates as a pseudo ground truth. 6. Use these new model parameters to repeat the process from step 1.

UR2iKiD [47] attempt to circumvent learning feature detection directly by extracting feature locations out of the feature map used to calculate descriptors. DISK [43] and Reinforced Feature Point [6] utilize reinforcement learning, with DISK using depth and pose to check whether matches are valid without any keypoints localization loss and Reinforced Feature Points only using the pose to evaluate the estimate.

Expectation Maximization in Deep Learning. Expectation Maximization (EM) being a greedy optimization framework is not new to deep learning. Multiple methods have introduced random sampling into their methods, allowing sampling the output distribution and performing something similar to EM. One such method is variational autoencoders [22], whose optimization can be formulated as an EM algorithm where the latent variable is the learned embedding [27]. Another instance is Bayesian neural networks [19], for which applying the EM algorithm is straightforward.

At a broader level, there are methods similar to ours that do not fall under the label of EM. For methods that cannot output "well-calibrated" probabilistic predictions, there exist similar approaches under the label "wrapper" methods by taxonomists [44]. Wrapper methods are model agnostic methods that alternate between training classifiers on

pseudo-labeled data, then use the predictions of the resulting classifier to predict new pseudo-labels. Then, unrelated to deep learning, EM has been used to perform image segmentation [7].

3. SEDM Framework

The goal of SEDM is to find 3D points for which the 2D appearance is learnable by our detector model. The model can then be trained to detect these points and learn some kind of generalizable notion of what these points look like. We call the resulting detector SEDM, which we then pair with various descriptors and matchers for use in traditional feature pipelines. If we use an SfM pipeline, like COLMAP [41], the goal would be to retrieve the 3D points that SEDM was trying to detect.

The two following sections correspond to the soft repeatability estimation and prediction generations steps of Figure 2. Section 3.1 focuses on how the current model, which is initialized to have random weights, can be used to generate an estimate for the repeatability of 3D points. Section 3.2 focuses on how these values are transformed into the pseudo-ground truth to be fed to the loss function. Together, these two steps for the expectation step of SEDM, with the maximization step being performed by typical deep learning methods.

3.1. Soft Repeatability Calculation

As we introduced in Section 1, repeatability is tied to some reprojection error threshold. However, if the underlying geometry of the scene is known, it is more convenient to tie repeatability to some projection error threshold in 3D space rather than reprojection error in image space. This allows us to discretize 3D space into voxels representing the different features the detector is possibly trying to localize. We can then calculate the repeatability of each spot in 3D space by counting the number of times it is detected, as shown in the Expectation Step in Figure 2. This gives us an improved estimate of the repeatability for each 3D point, which we can then leverage to improve the model, as shown in the Maximization Step in Figure 2. We can then iterate over these two steps, which is the essence of an EM algorithm.

The process of evaluating the repeatability of these points is relatively straightforward if we have a model of the environment being photographed and the exact pose of each image. One key detail that makes this process tractable is that our definition of repeatability is defined for some radius. If we fix this radius, we can approximately calculate repeatability by discretizing space into voxels, which we store in an octree for efficiency.

We begin our proposed method by first running the model, which is initialized with random weights, to produce a heatmap for each of the training set images associated with an octree. We then calculate a soft repeatability associated with each voxel in 3D space by projecting the heatmap values onto the voxelized 3D model, as can be seen in Step 2 of Figure 2. For each of these voxels, we accumulate the sum of heatmap scores and the number of rays that hit it, which allows us to calculate an average over these scores. We call this average the soft repeatability, to be compared with the average across indicator functions for some threshold. Since this projection process is expensive, performing it for multiple thresholds would be far too costly. Once we have this soft repeatability value for each voxel in 3D space, we project it back into 2D image space using a similar operation, as seen in Step 3 of Figure 2.

3.2. Prediction Generation

These soft repeatability could be fit with the model using an L_2 loss. However, there are a few more constraints on the problem than simply repeatability, most prominently that the points in 3D space must be sparse (for matching). Although we could perform this operation in 3D space, we found that filtering out edges, which are hard to match but highly repeatable, improved performance. That is why, in Step 4 of Figure 2, we convert the soft repeatability maps into a binary mask for each image, with sparse ones representing estimated locations of the ground truth feature locations. This prediction generation step could also be thought

of as part of the expectation step, with the pseudo-ground truth it generates being what induces a log-likelihood function using the cross entropy function.

$$L(x, y) = - \sum_{i=1}^n \sum_{j=1}^m y_{ij} \log x_{ij} + (1 - y_{ij}) \log(1 - x_{ij})$$

To produce this binary mask, we filter out edges, apply non-maximal suppression, then threshold the image. To filter out the edges, we filter out regions where the minor eigenvalue of the Hessian of the image, which we denote $Ds(x) \in \mathbb{R}^{2 \times 2}$, $s \in \mathbb{R}^2$, is less than some threshold.

$$\lambda_{\min} = \frac{\text{trace}(Ds(x)) - \sqrt{\text{trace}^2(Ds(x)) - 4\det(Ds(x))}}{2}$$

According to Harris and Stephen [15], this should only filter out flat regions, but it works because it negatively biases edges, which is enough for SEDM to remove them. In addition, it also scales with the repeatability score when at pointy locations, which allows us to threshold for both edge removal and retrieving a lower number of points at the same time. Non-maximal suppression, which finds local minima within a defined radius, was applied to this map of minor eigenvalues to find sparse points. Finally, the points are thresholded using a set threshold calculated before training starts to produce a desired number of points on a portion of the training set. We then train the model by maximizing this log-likelihood function, seen in Step 5, before using this trained model to produce new estimates in Step 6.

4. Implementation

For the model architecture, we tested KeyNet [5], SuperPoint [10], and a miniaturized UNet [33]. Both SuperPoint and mini-UNet converged while KeyNet very visibly failed to do so. Since the SuperPoint architecture was also capable of outputting descriptors if we had trained it, we focus on presenting the results for the SuperPoint architecture. For the descriptor and matcher, we use three combinations: HardNet [28] and the brute force matcher, original SuperPoint descriptor and the brute force matcher, and the original SuperPoint descriptor with SuperGlue [36], which is a graph neural network matcher.

4.1. Training

For training, we added Batch Normalization [17] operations to SuperPoint that seem to be essential for training. For each iteration, SuperPoint was trained for 300 epochs, although our experiments with other networks showed convergence using 50 epochs. Non-maximal suppression during training had radius 6 to discourage edges and 3 during testing to avoid missing keypoints. Points around a border with size 4 pixels of the output were not trained and

were omitted during testing because of issues caused by padding. When training SuperPoint, a cellwise suppression method, where only one keypoint was selected in each 8×8 cell was applied to match the softmax cells in the output of SuperPoint. The number of desired keypoints was changed every third iteration to follow the sequence [2000, 1700, 1200] to anneal over the number of keypoints. The output threshold was set to 0.025. Training was performed using PyTorch [30] on 480×480 images with a batch size of 32. We used the Adam [21] optimizer with $lr = 0.0001, \beta = (0.9, 0.999)$. Images were augmented using the ImgAug [20] library to apply random Gaussian blur, salt and pepper noise, random linear contrast, additive Gaussian noise, brightness variation, JPEG compression, and random affine and perspective transformations.

4.2. System Runtime

Our use of off the shelf models allows us to compute system runtime using their metrics. When using SuperPoint descriptors, we must run the same model architecture twice, once with our weights and once with the original author’s. According to [10], this gives us a runtime of 23.65 ms, or 42 FPS on a Titan X GPU at a resolution of 480×640 . For HardNet, the runtime is dependent on the number of descriptors extracted, with Mishchuk et al. [28] reporting a runtime of 1 ms on low end GPUs, but we obtain a runtime of 3 ms per a descriptor when extracting patches in accounted for on an Nvidia GTX1060.

4.3. Training Dataset

LEM requires that the training dataset have precise, dense depth that aligns with the visual images, as well as accurate pose. To obtain training data with these characteristics, we leverage both synthetic data generated from modeled scenes and data re-rendered from captured real-world data. We did not use MegaDepth [24] because of the methods they used to close holes in the depth maps could cause discrepancies between the visual appearance and the geometry of the scene. The Unreal Engine has a large marketplace of 3D scenes that are textured and illuminated, as well as photorealistic rendering techniques. By leveraging the UnrealCV plugin [31], which allows to capture color and depth from the Unreal Engine, we were able to capture photos with known underlying geometry. We used the following environments: 2 small rooms named RealisticRendering and Archviz Interior by Epic Games, 3 interiors of buildings as part of the Archinteriors Vol 2 by Evermotion, an Urban City model by PolyPixel and a forest biome with scanned assets by Tirido. We also selected 7 high quality scenes from the BlendedMVS [48] dataset, which is a synthetic dataset that utilizes the SfM reconstructions to render photorealistic images that match the underlying geometry. Together, these two datasets totaled in 45k images with

640×480 resolution.

4.4. Octrees

The depth images and their pose were then used to compile a 3D voxel map of the environment with voxel size such that the spatial resolution of the voxels is equal to the projected pixel size for most pixels. When raycasting from the image to the octree for either projection and reprojection, the raycasting is performed with random subpixel coordinates 5 times for each pixel. To prevent issues with overly large voxels, parts of the ground truth where the voxels were larger than 2 pixels were masked out.

5. Experiments

We test on the HPatches[4] Mean Matching Accuracy (MMA) using the code provided by Dusmanu et al. [11] as it is a popular and fast benchmark for detectors, used in [32] [5] [47][26][6], and more. However, according to a survey by Schonberger et al., improvements in metrics like MMA [42], which are designed to evaluate certain characteristics of feature extraction pipelines, often don’t translate to improvements later on in the pipeline. To better evaluate this performance later in the pipeline, we perform an SfM benchmark using COLMAP, very similar to how it was performed in the survey by Schonberger et al. We also evaluate on the long-term Visual Localization Benchmark [37], which is a service provided by the website `visuallocalization.net` which evaluates pose localization error at different thresholds for submitted pose estimates.

To select which methods to compare against, we chose the state of the art detector Superpoint, as well as a newer method, R2D2 [32]. R2D2 also gives good contrast as it is a method that focuses on the repeatability of feature detection as well as reliability of those features being matched, rather than optimizing directly for repeatability as we do. We also picked some popular methods to make our benchmarking results more easily comparable with other benchmarks. We also tested two variants of descriptors designed for SIFT: RootSIFT [3] and HardNet [28]. We do not yet have access to the training code of SuperGlue, so we were not able to provide SuperGlue matching for other descriptors.

5.1. Image Matching

This test uses 56 image sequences with viewpoint change sequences in planar environments with no illumination change and 52 sequences featuring illumination change with no viewpoint change from the HPatches dataset [4]. The first image is matched against all others in the sequence, and the reprojection error is obtained using the known homography between pairs. The number of pairs with error less than a varying threshold is then used to obtain an accuracy score. HardNet is omitted from the comparison be-

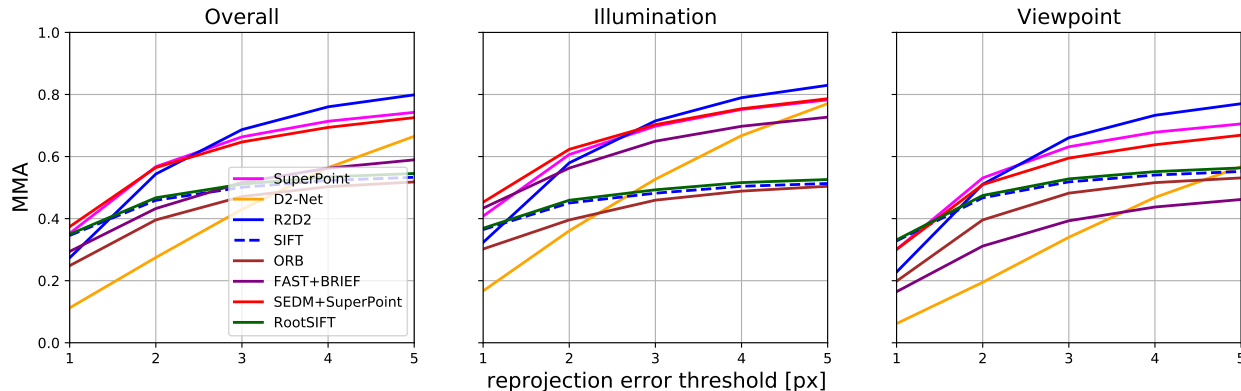


Figure 3. Graph of mean matching accuracy (MMA) at different maximum reprojection error thresholds for which a pair of points would be considered a match. For most applications, a reprojection error greater than 1 is considered poor.

cause it was trained on HPatches [28]. This test has its limitations, as the planar viewpoint changes make the viewpoint change results hard to compare to the real world.

The results are shown in Figure 3. One odd thing about this test is the range over which the reprojection error is allowed. Most applications of image features tend to minimize reprojection error, so having significant error in the localization of the keypoints can cause issues in many algorithms [1]. For many applications, reprojection error over a pixel is significant, and we shrink the range to $[1, 5]$ to better reflect this. That said, our method performs only slightly better than SuperPoint at relevant thresholds, but not significantly. This makes sense because SuperPoint was trained purely on homographies, which is equivalent to how viewpoint invariance is represented in HPatches. We do outperform SuperPoint by a slim margin in illumination, which shows that training on synthetic lighting change is potentially more effective than image augmentations that simulate lighting change.

5.2. Visual Localization

We utilize *The Visual Localization Benchmark* service [37] provided by¹ to evaluate the poses we predict using the HLOC [35] toolkit. This benchmark tests the ability of a method to localize a set of query images using a set of database images. To run this benchmark, image retrieval is first performed using either NetVLAD [2] to extract the top 50 pairs within the database images, then features are extracted and matched across these images. These matches and features are then passed to COLMAP [41] for either 3D reconstruction or 3D triangulation, with triangulation being used if the pose of the database images is provided to triangulate the points from each camera. The query images are then matched to the top 50 image retrieval pairs with the

database, and the location of the matched points is used to determine the location of the query image.

The distance and angular difference between the predicted poses and the ground truth poses is then calculated, and the percentage of images that lie within the thresholds of $(0.25 \text{ m}, 2^\circ)$, $(0.5 \text{ m}, 5^\circ)$, $(5 \text{ m}, 10^\circ)$. The results are reported in Table 1. The top results with code or a paper linked are reported. Although our method remain competitive in this benchmark, it does not surpass SuperPoint+SuperGlue. Due to thresholds for localization accuracy are rather wide and conditions are difficult, it seems likely that the combination of SuperGlue not being trained on SEDM keypoints and keypoint localization accuracy being less important made our results less competitive in this benchmark.

5.3. 3D Reconstruction

Just like in the survey by Schonburger et al. [42], we use COLMAP [41] to perform sparse 3D reconstruction and report the statistics for the reconstruction. We performed reconstruction for Aachen Day and Night [39], Alamo and Tower of London [46], and South Building [14]. From these statistics, we are able to evaluate the quality of the reconstruction and therefore the detectors. Primarily, we will focus on mean reprojection error and number of registered poses because they are more universally useful when SfM is performed [13]. The mean reprojection error, which we shortened to reproj. error, is the residual error after minimization between the predicted detection location and the reprojected 3D point in image space. We use this as a best effort metric for the precision with which the feature detector is able to localize the corresponding 3D point. However, it has its limitations, like issues with the camera model, possible local minima in the bundle adjustment process, and the possibility of reaching global minima at an incorrect solution. The 3D point is likely not even located on the surface

¹<https://www.visuallocalization.net/benchmark/>

Aachen Day-Night						
Method	Day			Night		
	(0.25 m, 2°)	(0.5 m, 5°)	(5 m, 10°)	(0.25 m, 2°)	(0.5 m, 5°)	(5 m, 10°)
SuperPoint + SuperGlue	89.6	95.4	98.8	86.7	93.9	100.0
SuperPoint + SuperGlue (our run)	89.4	95.8	98.8	85.7	92.9	100.0
SEDM + Superpoint + SuperGlue (ours)	88.6	95.1	98.7	83.7	91.8	99.0
Kapture + R2D2 + APGeM[16]	88.7	95.8	98.8	81.6	88.8	96.9
ONavi [12]	85.7	93.7	98.9	81.6	91.8	100.0

RobotCar Seasons						
SuperPoint + SuperGlue Multi Camera	55.7	82.0	97.6	37.7	71.5	91.1
SuperPoint + SuperGlue	56.9	81.7	98.1	33.3	65.9	88.8
Kapture + R2D2 + APGeM[16]	55.1	82.1	97.3	28.8	58.8	89.4
SEDM + Superpoint + SuperGlue (ours)	53.9	80.0	96.4	24.7	50.5	82.6
Geometric Prior Guided Camera [38]	57.3	81.7	97.6	8.0	21.6	40.7

Table 1. Visual localization results from `visuallocalization.net`, sorted by average accuracy. Each value is the percentage of images registered within different thresholds of allowed translation and orientation error.

The number of registered poses is the number of poses that the SfM process was able to find a pose for, which is often a very important down stream metric that seems to be affected by the detector. The number of sparse points obtained is hard to use to infer detector characteristics. The mean track length is the number of observations divided by the number of sparse points. The mean features is the average number of features output by the detector. We utilize the HLOC [35] toolbox to perform feature extraction and matching for all feature pipelines.

There are a few changes to keep the scope of the testing feasible. We limit the number of keypoints to 4096 to keep the complexity and RAM usage down. Some methods, like SIFT and FAST, would detect $>10k$ points occasionally. This allowed us to use HardNet as a descriptor for SIFT in a reasonable amount of time. We also limit the largest dimension of each image to 1600 and don't perform per a dataset tuning of parameters for any method.

The results are presented in Table 2. As in the original survey [42], SIFT with SIFT or RootSIFT features results in the lowest mean reprojection error. However, there are a few interesting observations we need to look at. First, SuperGlue does not seem to perform well for mean reprojection error. We hypothesize that this is because SuperGlue bypasses the MSAC process that filters out bad matches. While it seems to register more images and triangulate more points, it also has difficulty filtering out outliers when compared to brute force matching + MSAC. Second, both HardNet and RootSIFT, which are supposed to increasing matching performance for SIFT, increase the mean reprojection error on most of the datasets, but doesn't do the same for SEDM. In fact, the matching algorithm has a large impact on the mean reprojection error, which tells us that this metric is very difficult to read as purely a measure of keypoint

localization accuracy.

Since reprojection error is an average over hundreds images and thousands of points, the distribution it comes from is approximately normal by the Central Limit Theorem. This means that we can perform a two tailed paired T-test at $\alpha = 0.05$ on the mean difference between the reprojection error of our method versus SIFT, SuperPoint, and R2D2, with each dataset constituting a data point. We fail to reject the null hypothesis, that the difference between SEDM and another method is 0, for the SuperPoint, R2D2, and SIFT, when using the nearest neighbor matcher and MSAC. There is a 95% chance that the true mean of the mean reprojection error when using SEDM decreases by $0.15 \pm 0.11px$ when compared to SuperPoint, $-0.38 \pm 0.23px$ when compared to R2D2, and increased by $0.30 \pm 0.09px$ when compared to SIFT. When using SuperGlue, we accept the null hypothesis, that the detector has no effect on the mean reprojection error.

6. Discussion and Conclusion

We have presented SEDM, a technique that allows us to optimize for feature repeatability in 3D space using a soft expectation function and deep learning based maximization. This optimization produces a detector as well as a map of the repeatability of the features the detector predicts. We then paired this detector with various descriptors and matching methods so we could benchmark the performance on 3 different tests.

If we accept mean reprojection error as a best effort metric of evaluating reconstruction performance, then we can claim that there is a 95% chance that we are able to improve upon the state of the art deep learning methods, SuperPoint and R2D2, in the domain of reconstruction. How-

	Detector	Descriptor	Matcher	#Sparse Points	#Observations	Track Length	Avg. #Features	#Registered	Reproj. Err.	
Aachen Day Night Min: 1024x768 Max: 1200x1600 Tranpose sizes too	SIFT	SIFT	NN	885211	4462937	5.042	3986	4328/4328	0.817	
		RootSIFT	NN	951176	4801804	5.048	3986	4328/4328	0.839	
		HardNet	NN	560062	3281185	5.859	3986	4328/4328	0.782	
		SuperPoint	SuperGlue	1340981	8293771	6.185	3761	4328/4328	1.402	
		R2D2	R2D2	NN	1080662	8094569	7.490	4096	4328/4328	1.400
		FAST	BRIEF	NN	403725	1956711	4.847	1875	4328/4328	1.177
		ORB	ORB	NN	786149	4077735	5.187	4091	4328/4328	1.058
		Superpoint	SuperPoint	NN	1276720	7790523	6.102	3704	4328/4328	1.160
			SuperPoint	SuperGlue	1499782	10146354	6.765	3704	4328/4328	1.294
		SEDM(ours)	SuperPoint	NN	1097518	6881319	6.270	3665	4328/4328	1.014
		HardNet	NN	1304537	8136450	6.237	3665	4328/4328	1.012	
		SuperPoint	SuperGlue	1543668	10280681	6.660	3665	4328/4328	1.240	
Alamo Min: 122x139 Max: 1600x3246	SIFT	SIFT	NN	96186	740572	7.699	3472	713/2915	0.652	
		RootSIFT	NN	103092	799367	7.754	3472	728/2915	0.688	
		HardNet	NN	121669	1020548	8.388	3472	888/2915	1.084	
		SuperPoint	SuperGlue	183386	1653725	9.018	3472	1024/2915	1.322	
		R2D2	R2D2	NN	145740	1535147	10.533	4077	1025/2915	1.205
		FAST	BRIEF	NN	73600	670567	9.111	2885	682/2915	0.963
		ORB	ORB	NN	100421	953868	9.499	2794	641/2915	0.949
		SuperPoint	SuperPoint	NN	75815	953055	12.571	2794	883/2915	1.102
			SuperPoint	SuperGlue	222815	1911333	8.578	2794	1279/2915	1.231
		SEDM(ours)	Superpoint	NN	83610	1155235	13.817	2712	890/2915	1.013
		HardNet	NN	135674	1487105	10.961	2712	963/2915	1.025	
		Superpoint	SuperGlue	233055	2156254	9.252	2712	1253/2915	1.214	
Tower of London Min: 320x320 Max: 1600x2133	SIFT	SIFT	NN	98595	529582	5.371	3446	542/1576	0.645	
		RootSIFT	NN	110426	591559	5.357	3446	603/1576	0.667	
		HardNet	NN	102714	700781	6.823	3446	646/1576	1.000	
		Superpoint	SuperGlue	151699	1180888	7.784	3260	835/1576	1.284	
		R2D2	R2D2	NN	98593	978208	9.922	4060	763/1576	1.212
		FAST	BRIEF	NN	68277	416780	6.104	2868	498/1576	0.916
		ORB	ORB	NN	46264	287187	6.208	3962	387/1576	0.900
		SuperPoint	SuperPoint	NN	73390	630968	8.597	2840	708/1576	1.016
			SuperPoint	SuperGlue	163976	1235694	7.536	2840	948/1576	1.194
		SEDM(ours)	Superpoint	NN	95428	794899	8.330	2697	721/1576	0.916
		HardNet	NN	139100	1053624	7.575	2697	755/1576	0.900	
		Superpoint	SuperGlue	186062	1417816	7.620	2697	930/1576	1.115	
South Building 3072x3204	SIFT	SIFT	NN	40985	227419	5.549	4096	128/128	0.429	
		RootSIFT	NN	41663	231821	5.564	4096	128/128	0.441	
		HardNet	NN	24828	180002	7.250	4096	128/128	0.541	
		SuperPoint	SuperGlue	41556	290447	6.989	4096	128/128	0.875	
		R2D2	R2D2	NN	45955	267147	5.813	4096	128/128	1.430
		ORB	ORB	NN	26590	101056	3.801	3998	102/128	1.272
		FAST	BRIEF	NN	34911	210196	6.021	3798	128/128	0.876
		SuperPoint	SuperPoint	NN	44729	278251	6.221	4056	128/128	1.063
			SuperPoint	SuperGlue	56136	355468	6.332	4056	128/128	1.190
		SEDM(ours)	Superpoint	NN	50626	312051	6.164	4096	128/128	0.780
		HardNet	NN	58136	347119	5.971	4096	128/128	0.810	
		Superpoint	SuperGlue	59116	381247	6.449	4096	128/128	0.941	

Table 2. Reconstruction results obtained using COLMAP and the HLOC toolkit. Best results are bolded.

ever, SEDM still lags behind SIFT by a significant margin. In the realm of Visual Localization, our method performs at a state of the art level, reaching top 4 average localization performance in Aachen Day-Night and RobotCar Seasons despite the lack of finetuning of the matcher. As such, we conclude that optimizing repeatability of features in 3D space is an effective method of training an image feature detector and leads to more accurate keypoint localization in the context of 3D reconstruction, but that there seems to be more work needed before deep learning detectors fully surpass traditional techniques.

6.1. Future Work

We believe that it is necessary to investigate better sub-pixel detection methods. It is important to remember that simply scaling up the image to achieve subpixel accuracy is not an efficient solution because, although our compute power has increased, so too has camera resolution and the number of images we wish to process. Another potential area for improvement is our prediction generation method in Section 3.2. Our keypoint selection process is not scale invariant, which led to some performance deficits. Our edge heuristic, designed to select for matchable points, could also potentially be replaced with a reliability filter like the one

suggested by R2D2 [32]. A reimplementation of the training routine for SuperGlue would allow better comparisons to SuperPoint, as there seems to be a gap in performance caused by lack of finetuning on our detector. When comparing the number of images registered for Alamo and Tower of London, LEDM registers more images compared to SuperPoint without SuperGlue, but the reverse is true when SuperGlue is used. There is also the practical need to train descriptor for our model to improve runtime performance, but the descriptors need to be trained separately on a large dataset.

References

- [1] Alex M Andrew. Multiple view geometry in computer vision. *Kybernetes*, 2001.
- [2] Relja Arandjelovic, Petr Gronat, Akihiko Torii, Tomas Pajdla, and Josef Sivic. NetVLAD: CNN architecture for weakly supervised place recognition. In *Proceedings of the IEEE conference on computer vision and pattern recognition*, pages 5297–5307, 2016.
- [3] Relja Arandjelović and Andrew Zisserman. Three things everyone should know to improve object retrieval. In *2012 IEEE Conference on Computer Vision and Pattern Recognition*, pages 2911–2918. IEEE, 2012.
- [4] Vassileios Balntas, Karel Lenc, Andrea Vedaldi, and Krystian Mikolajczyk. HPatches: a benchmark and evaluation of handcrafted and learned local descriptors. In *Proceedings of the IEEE conference on computer vision and pattern recognition*, pages 5173–5182, 2017.
- [5] Axel Barroso-Laguna, Edgar Riba, Daniel Ponsa, and Krystian Mikolajczyk. KeyNet: keypoint detection by handcrafted and learned cnn filters. In *Proceedings of the IEEE International Conference on Computer Vision*, pages 5836–5844, 2019.
- [6] Aritra Bhowmik, Stefan Gumhold, Carsten Rother, and Eric Brachmann. Reinforced feature points: Optimizing feature detection and description for a high-level task. In *Proceedings of the IEEE/CVF conference on computer vision and pattern recognition*, pages 4948–4957, 2020.
- [7] Chad Carson, Serge Belongie, Hayit Greenspan, and Jitendra Malik. Blobworld: Image segmentation using expectation-maximization and its application to image querying. *IEEE Transactions on pattern analysis and machine intelligence*, 24(8):1026–1038, 2002.
- [8] Peter Hviid Christiansen, Mikkel Fly Kragh, Yury Brodskiy, and Henrik Karstoft. Unsuperpoint: End-to-end unsupervised interest point detector and descriptor. *arXiv preprint arXiv:1907.04011*, 2019.
- [9] Titus Cieslewski, Konstantinos G Derpanis, and Davide Scaramuzza. Sips: Succinct interest points from unsupervised inlierness probability learning. In *2019 International Conference on 3D Vision (3DV)*, pages 604–613. IEEE, 2019.
- [10] Daniel DeTone, Tomasz Malisiewicz, and Andrew Rabinovich. SuperPoint: self-supervised interest point detection and description. *CoRR*, abs/1712.07629, 2017.
- [11] Mihai Dusmanu, Ignacio Rocco, Tomas Pajdla, Marc Pollefeys, Josef Sivic, Akihiko Torii, and Torsten Sattler. D2-Net: a trainable cnn for joint detection and description of local features. *arXiv preprint arXiv:1905.03561*, 2019.
- [12] Huanhuan Fan, Yuhao Zhou, Ang Li, Shuang Gao, Jijun-nan Li, and Yandong Guo. Visual localization using semantic segmentation and depth prediction. *arXiv preprint arXiv:2005.11922*, 2020.
- [13] Wolfgang Förstner and Bernhard P Wrobel. *Photogrammetric computer vision*. Springer, 2016.
- [14] Christian Hane, Christopher Zach, Andrea Cohen, Roland Angst, and Marc Pollefeys. Joint 3d scene reconstruction and class segmentation. In *Proceedings of the IEEE Conference on Computer Vision and Pattern Recognition*, pages 97–104, 2013.
- [15] Christopher G Harris, Mike Stephens, et al. A combined corner and edge detector. In *Alvey vision conference*, volume 15, pages 10–5244. Citeseer, 1988.
- [16] Martin Humenberger, Yohann Cabon, Nicolas Guerin, Julien Morat, Jérôme Revaud, Philippe Rerole, Noé Pion, Cesar de Souza, Vincent Leroy, and Gabriela Csurka. Robust image retrieval-based visual localization using kapture. *arXiv preprint arXiv:2007.13867*, 2020.
- [17] Sergey Ioffe and Christian Szegedy. Batch normalization: Accelerating deep network training by reducing internal covariate shift. In *International conference on machine learning*, pages 448–456. PMLR, 2015.
- [18] Yuhe Jin, Dmytro Mishkin, Anastasiia Mishchuk, Jiri Matas, Pascal Fua, Kwang Moo Yi, and Eduard Trulls. Image matching across wide baselines: From paper to practice. *International Journal of Computer Vision*, pages 1–31, 2020.
- [19] Laurent Valentin Jospin, Wray Buntine, Farid Boussaid, Hamid Laga, and Mohammed Bannamoun. Hands-on bayesian neural networks—a tutorial for deep learning users. *arXiv preprint arXiv:2007.06823*, 2020.
- [20] Alexander B. Jung. imgaug. <https://github.com/aleju/imgaug>, 2018. [Online; accessed 30-Oct-2018].
- [21] Diederik P Kingma and Jimmy Ba. Adam: A method for stochastic optimization. *arXiv preprint arXiv:1412.6980*, 2014.
- [22] Diederik P Kingma and Max Welling. Auto-encoding variational bayes. *arXiv preprint arXiv:1312.6114*, 2013.
- [23] Karel Lenc and Andrea Vedaldi. Learning covariant feature detectors. In *European conference on computer vision*, pages 100–117. Springer, 2016.
- [24] Zhengqi Li and Noah Snavely. MegaDepth: learning single-view depth prediction from internet photos. In *Proceedings of the IEEE Conference on Computer Vision and Pattern Recognition*, pages 2041–2050, 2018.
- [25] David G Lowe. Distinctive image features from scale-invariant keypoints. *International journal of computer vision*, 60(2):91–110, 2004.
- [26] Zixin Luo, Lei Zhou, Xuyang Bai, Hongkai Chen, Jiahui Zhang, Yao Yao, Shiwei Li, Tian Fang, and Long Quan. ASLFeat: learning local features of accurate shape and localization. In *Proceedings of the IEEE/CVF Conference on Computer Vision and Pattern Recognition*, pages 6589–6598, 2020.

- [27] David McAllester. VAE = EM. Machine Thoughts. <https://machinethoughts.wordpress.com/2017/10/02/vae-em/>. (Accessed Mar 2021).
- [28] Anastasiya Mishchuk, Dmytro Mishkin, Filip Radenovic, and Jiri Matas. Working hard to know your neighbor's margins: Local descriptor learning loss. *arXiv preprint arXiv:1705.10872*, 2017.
- [29] Yuki Ono, Eduard Trulls, Pascal Fua, and Kwang Moo Yi. Lf-net: Learning local features from images. *arXiv preprint arXiv:1805.09662*, 2018.
- [30] Adam Paszke, Sam Gross, Francisco Massa, Adam Lerer, James Bradbury, Gregory Chanan, Trevor Killeen, Zeming Lin, Natalia Gimelshein, Luca Antiga, Alban Desmaison, Andreas Kopf, Edward Yang, Zachary DeVito, Martin Raison, Alykhan Tejani, Sasank Chilamkurthy, Benoit Steiner, Lu Fang, Junjie Bai, and Soumith Chintala. Pytorch: An imperative style, high-performance deep learning library. In H. Wallach, H. Larochelle, A. Beygelzimer, F. d'Alché-Buc, E. Fox, and R. Garnett, editors, *Advances in Neural Information Processing Systems 32*, pages 8024–8035. Curran Associates, Inc., 2019.
- [31] Weichao Qiu, Fangwei Zhong, Yi Zhang, Siyuan Qiao, Zihao Xiao, Tae Soo Kim, Yizhou Wang, and Alan Yuille. UnrealCV: virtual worlds for computer vision. *ACM Multimedia Open Source Software Competition*, 2017.
- [32] Jérôme Revaud, Philippe Weinzaepfel, César Roberto de Souza, Noé Pion, Gabriela Csurka, Yohann Cabon, and Martin Humenberger. R2D2: repeatable and reliable detector and descriptor. *CoRR*, abs/1906.06195, 2019.
- [33] Olaf Ronneberger, Philipp Fischer, and Thomas Brox. U-net: Convolutional networks for biomedical image segmentation. In *International Conference on Medical image computing and computer-assisted intervention*, pages 234–241. Springer, 2015.
- [34] Edward Rosten and Tom Drummond. Machine learning for high-speed corner detection. In *European conference on computer vision*, pages 430–443. Springer, 2006.
- [35] Paul-Edouard Sarlin, Cesar Cadena, Roland Siegwart, and Marcin Dymczyk. From coarse to fine: Robust hierarchical localization at large scale. In *Proceedings of the IEEE Conference on Computer Vision and Pattern Recognition*, pages 12716–12725, 2019.
- [36] Paul-Edouard Sarlin, Daniel DeTone, Tomasz Malisiewicz, and Andrew Rabinovich. SuperGlue: learning feature matching with graph neural networks. *2020 IEEE/CVF Conference on Computer Vision and Pattern Recognition (CVPR)*, pages 4937–4946, 2020.
- [37] Torsten Sattler, Will Maddern, Carl Toft, Akihiko Torii, Lars Hammarstrand, Erik Stenborg, Daniel Safari, Masatoshi Okutomi, Marc Pollefeys, Josef Sivic, et al. Benchmarking 6dof outdoor visual localization in changing conditions. In *Proceedings of the IEEE Conference on Computer Vision and Pattern Recognition*, pages 8601–8610, 2018.
- [38] Torsten Sattler, Will Maddern, Carl Toft, Akihiko Torii, Lars Hammarstrand, Erik Stenborg, Daniel Safari, Masatoshi Okutomi, Marc Pollefeys, Josef Sivic, et al. Benchmarking 6dof outdoor visual localization in changing conditions. In *Proceedings of the IEEE Conference on Computer Vision and Pattern Recognition*, pages 8601–8610, 2018.
- [39] Torsten Sattler, Tobias Weyand, Bastian Leibe, and Leif Kobbelt. Image retrieval for image-based localization revisited. In *BMVC*, volume 1, page 4, 2012.
- [40] Nikolay Savinov, Akihito Seki, Lubor Ladicky, Torsten Sattler, and Marc Pollefeys. Quad-networks: unsupervised learning to rank for interest point detection. In *Proceedings of the IEEE conference on computer vision and pattern recognition*, pages 1822–1830, 2017.
- [41] Johannes Lutz Schönberger and Jan-Michael Frahm. Structure-from-motion revisited. In *Conference on Computer Vision and Pattern Recognition (CVPR)*, 2016.
- [42] Johannes L. Schonberger, Hans Hardmeier, Torsten Sattler, and Marc Pollefeys. Comparative evaluation of hand-crafted and learned local features. In *Proceedings of the IEEE conference on computer vision and pattern recognition*, pages 1482–1491, 2017.
- [43] Michał J Tyszkiewicz, Pascal Fua, and Eduard Trulls. DISK: Learning local features with policy gradient. *arXiv preprint arXiv:2006.13566*, 2020.
- [44] Jesper E Van Engelen and Holger H Hoos. A survey on semi-supervised learning. *Machine Learning*, 109(2):373–440, 2020.
- [45] Yannick Verdie, Kwang Yi, Pascal Fua, and Vincent Lepetit. TILDE: a temporally invariant learned detector. In *Proceedings of the IEEE Conference on Computer Vision and Pattern Recognition*, pages 5279–5288, 2015.
- [46] Kyle Wilson and Noah Snavely. Robust global translations with 1dsfm. In *Proceedings of the European Conference on Computer Vision (ECCV)*, 2014.
- [47] Tsun-Yi Yang, Duy-Kien Nguyen, Huub Heijnen, and Vasileios Balntas. UR2KiD: unifying retrieval, keypoint detection, and keypoint description without local correspondence supervision. *arXiv preprint arXiv:2001.07252*, 2020.
- [48] Yao Yao, Zixin Luo, Shiwei Li, Jingyang Zhang, Yufan Ren, Lei Zhou, Tian Fang, and Long Quan. BlendedMVS: a large-scale dataset for generalized multi-view stereo networks, 2020.
- [49] Kwang Moo Yi, Eduard Trulls, Vincent Lepetit, and Pascal Fua. LIFT: learned invariant feature transform. In *European Conference on Computer Vision*, pages 467–483. Springer, 2016.